

Performance of New Control Strategy of Dual Stator Induction Generator System Applied in Wind Power Generation

Fatima Ameur^{a,b,1,*}, Katia Kouzi^{b,2}, Khadidja Ameur^{c,3}

^a Department of Electronics and Telecommunications, Ouargla University, Ouargla 30000, Algeria

^b Laboratoire des Semiconducteurs et Matériaux Fonctionnels, Université Amar Telidji de Laghouat, BP 37G Laghouat 03000, Algeria

^c Department of Informatique, Ouargla University, Ouargla 30000, Algeria

¹ Ameur.fatima@univ-ouargla.dz; ² Katia.Kouzi@gmail.com; ³ Ameur.khadidja@univ-ouargla.dz

* Corresponding Author

ARTICLE INFO

Article history

Received April 18, 2024

Revised May 21, 2024

Accepted May 31, 2024

Keywords

Dual Stator Induction

Generator,

Variable Speed Wind Turbine;

Direct Torque Flux Control;

AC/DC/AC PWM Converter;

Maximum Power Point

Tracking;

PI Controller

ABSTRACT

In order to improve the quality of energy and reduce the harmonics produced by the power electronics converters, it is proposed and developed in this article the direct torque control, in which the flux and torque are estimated from the only measurable electrical quantities. The direct torque control DTC method, to enhance the dynamic and static performances as well as the robustness of the control of the Wind Energy Conversion System (DSIG). DTC is a control technique that exploits the possibility of imposing torque and flux on alternating current machines in a decoupled manner, once powered by a voltage inverter without current regulation made by a feedback loop, ensuring a decoupling, similar to that obtained from a vector control. The technique involved rapid torque response, insensitivity to parametric variation, in particular the machine's rotor time constant and systematic suitability for control without speed sensor. The main function of the generator side controller is to track the maximum power through controlling the rotational speed of the wind turbine using PI controller. The performance and the effectiveness of the proposed control system are tested via simulation results in terms of reference tracking, and robustness against parameters variations of the DSIG. Simulation results for 1.5 MW DSIG control show robust with respect to the parametric variation 2 Rs, 1,5 Rs et 0.5 Rs, and fast dynamic behavior of system, with the temps of response is 0.02 s, active power extracted 0.15 MW with lambda 9 and Cp 0,5 that the wind turbine can operate at its optimum power point for a wide range of wind speed and power quality can be greatly improved.

This is an open-access article under the [CC-BY-SA](#) license.



1. Introduction

The recent trend indicates that wind energy will play a major role in meeting the future energy target worldwide [1], on the one hand to reduce dependence on fossil fuels and to minimize the negative impact of climate change on the other [2], [3]. Today, the development and multiplication of wind turbines has led electrical engineering researchers to conduct [4] investigations in order to improve the efficiency of electromechanical conversion [5] and the quality of the energy supplied

[6], [7]. Several electrical machines can be used to implement the electromechanical conversion, each of which presents different advantages and drawbacks [8]-[13].

In order to increase the power of a drive system Multi-phase induction [14] AC power machines appeared an ultimate solution [15]-[20]. Multiphase (more than three phases) drives have several advantages compared with conventional AC motors [21], such as reducing the amplitude and increasing the frequency of torque pulsations [22], reducing the rotor harmonic currents, reducing the current per phase without increasing the voltage per phase, and higher reliability [23]-[24]. By increasing the number of phases it is also possible to increase the power /torque per rms ampere for the same volume machine [25]-[27]. A common type of multi-phase machine is the dual stator induction machine (DSIM), also known as the six phase induction machine [28].

Generally, in a variable speed wind energy system [29], below rated wind velocity [30], the electrical torque is controlled in order to drive the system into an optimum speed for maximum energy conversion [31], [32].

One of the most common control methods for DSIG is vector control [33]-[36], in which the machine currents are decomposed into stators currents (torque, and flux) [37]-[40] and these two currents are controlled in the reference frame fixed to stator flux (or voltage) [41]-[46]. In this method, accurate value of machine parameters such as resistances and inductances are required and nonlinear operation of converter for tuning current controllers is not considered. So performance of vector control method is affected by changing machine parameters and operation condition [47], [48]. The direct torque control (DTC) is one of the actively researched control [49] scheme which is based on the decoupled control of flux and torque providing a very quick and robust response with a simple control construction in ac drives for improve energy quality and reduce harmonics produced by power electronics converters [47], [50]. In the mid 1980s, DTC of induction machine drives was developed [49]-[51].

DTC is a control technique exploiting the ability to impose torque and flux to AC machines in a decoupled way [47], [48], once supplied by a voltage inverter without current regulation made by a feedback loop, ensuring decoupling, similar to that obtained from a vector command [52]-[55]. This technique is used to calculate the stator flux and electromagnetic torque control quantities from the stator current measurements [56]-[59].

This is the purpose of our study on one of the renewable energies currently under development, wind energy. On the one hand, we will be interested in the current state of technological advances that have allowed the construction and proper functioning of wind turbines and their insertion in electricity production, the optimal design of a wind energy conversion system using a dual stator induction machine (DSIM).

This paper is constructed as follows: in Section 2, the modeling of the wind generator and the MPPT are presented. Section 3 deals with the Direct Torque control (DTC) of a DSIG. In Section 4, the performances of the proposed control are illustrated by some simulation results, Finally, some concluding remarks are given in Nomenclature.

1.1. Modeling of the Wind Turbine and Gearbox

Wind turbine mechanical power is expressed as follows [17] and [32]:

$$P_t = C_p(\lambda)\rho S V^3 \quad (1)$$

Where C_p is the power coefficient of the turbine, ρ is the air density, R is the blade length and V is the wind velocity. The turbine torque is the ratio of the out power to the shaft speed Ω_t , given by [27]:

$$T_t = \frac{P_t}{\Omega_t} \quad (2)$$

Is the product of the out power and the shaft speed Ω_t [31], [32], [36].

The turbine is usually connected to the generator shaft through a gearbox whose gear ratio is chosen to set the generator shaft speed within a desired range. After taking out the losses in the transmission, we can figure out how much force and speed the wind turbine has on its generator side of the gearbox:

$$T_g = \frac{T_t}{G}, \Omega_r = \frac{\Omega_t}{G} \quad (3)$$

Where the T_g driving is torque of the generator and Ω_r is the generator shaft speed. The captured wind power is not converted totally by the wind turbine. $C_p(\lambda)$ Give us the percentage converted which is function of the wind speed, the turbine speed and the pith angle of specific wind turbine blades [30].

Although this equation seems simple, C_p is dependent on the ratio λ between the turbine angular velocity Ω_t and the wind speed V . this ratio is called the tip speed ratio expressed by [30]:

$$\lambda = \frac{\Omega_t R}{V} \quad (4)$$

The areodynamique torque (wind) is determined the following equation [36], [17], [37]:

$$T_t = \frac{P_t}{\Omega_t} = C_p(\lambda) S \rho V^3 / 2 \Omega_t \quad (5)$$

The previous equations have established a functional block diagram model of the turbine. It indicates that the turbine rotation speed is controlled by the electromagnetic torque of the generator. The wind speed is deemed as a disruptive factor to this system (as illustrated in Fig. 1) The wind speed varies over time, and in order to ensure maximum capture of wind energy incident, the speed of the wind turbine should be adjusted permanently with that of the wind [37].

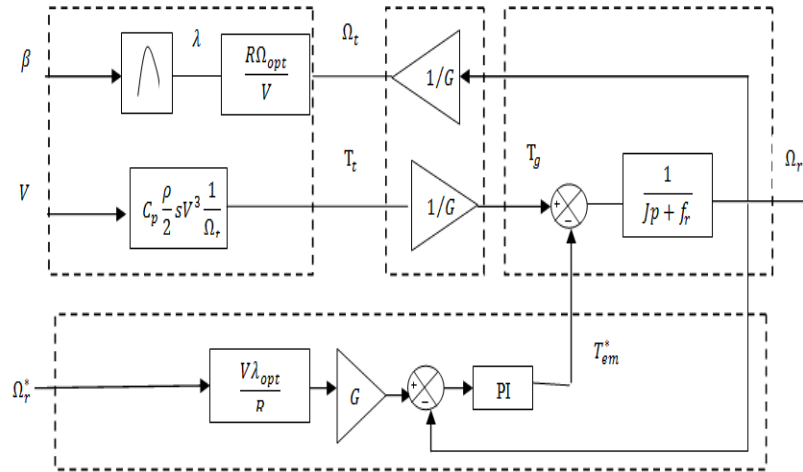


Fig. 1. The control of turbine

1.2. Dual Star Induction Generator Model

The dual star induction generator model consists of a squirrel cage rotor and a stator with two identical phase windings shifted by an electric angle of thirty degrees. To simplify the study of this machine, we adopt the following simplifying hypotheses [17], [37]:

Suppose that the structure of the machine is homogeneous, that is, the length of the gap is constant.

We also admit magneto motor force. that the voltages generated by each phase of the two armatures have a sinusoidal spatial distribution. The saturation of the magnetic circuit, hysteresis and eddy currents are negligible. The saturation of the magnetic circuit, hysteresis and eddy currents are negligible. The mutual leakage inductance common to both circuits (star 1 and star 2) is negligible. The machine is considered to work in a balanced diet.

The equivalent two-phase model of dual stator induction machine, represented in asynchronous frame (d, q) and expressed in state-space in the following form [37]:

$$[i] = [L]^{-1}\{[B][U] - \omega_{gl}[C][I] - [D][I]\} \quad (6)$$

Where:

$$\omega_{gl} = \omega_s - \omega_r; \omega_r = P * \Omega_r;$$

$$[U] = [V_{qs1} V_{ds1} V_{qs2} V_{ds2} V_{qr} V_{dr}]^t; [I] = [I_{qs1} I_{ds1} I_{qs2} I_{ds2} I_{qr} I_{dr}]^t; [\dot{I}] = \frac{d[I]}{dt};$$

$$[B] = \text{diag}[1 \ 1 \ 1 \ 1 \ 0 \ 0]$$

$$[C] = \begin{bmatrix} 0 & 0 & 0 & 0 & 0 & 0 \\ 0 & 0 & 0 & 0 & 0 & 0 \\ 0 & 0 & 0 & 0 & 0 & 0 \\ 0 & 0 & 0 & 0 & 0 & 0 \\ L_m & 0 & L_m & 0 & 0 & L_r + L_m \\ 0 & L_m & 0 & L_m & -(L_r + L_m) & 0 \end{bmatrix}$$

$$[L] = \begin{bmatrix} L_{s1} + L_m & 0 & L_m & 0 & L_m & 0 \\ 0 & L_{s1} + L_m & 0 & L_m & 0 & L_m \\ L_m & 0 & L_{s2} + L_m & 0 & L_m & 0 \\ 0 & L_m & 0 & L_{s2} + L_m & 0 & L_m \\ L_m & 0 & L_m & 0 & L_r + L_m & 0 \\ 0 & L_m & 0 & L_m & 0 & L_r + L_m \end{bmatrix}$$

$$[D] = \begin{bmatrix} R_{s1} & -\omega_s(L_{s1} + L_m) & 0 & -\omega_s L_m & 0 & -\omega_s L_m \\ \omega_s(L_{s1} + L_m) & R_{s1} & \omega_s L_m & 0 & \omega_s L_m & 0 \\ 0 & -\omega_s L_m & R_{s2} & -\omega_s(L_{s1} + L_m) & 0 & -\omega_s L_m \\ \omega_s L_m & 0 & \omega_s(L_{s1} + L_m) & R_{s2} & 0 & 0 \\ 0 & 0 & 0 & 0 & R_r & 0 \\ 0 & 0 & 0 & 0 & 0 & R_r \end{bmatrix}$$

The mechanical modeling part of the system is given by [31], [32], [36]:

$$J \frac{d\Omega_r}{dt} = T_g - T_{em} - f_r \Omega_r \quad (7)$$

With:

$$T_{em} = \left(\frac{p}{2}\right) \left(\frac{L_m}{L_{md} + L_r}\right) \left[(i_{qs1} + i_{qs2}) \varphi_{dr} - (i_{ds1} + i_{ds2}) \varphi_{qr} \right] \quad (8)$$

1.3. Grid Side Power Control

When the wind generator is in grid-connected control mode, all of its available power is fed into the grid. The (abc) synchronous frame's dc link voltage and inverter output currents are controlled by standard PI controllers. The reference reactive power Q needs to be zero in order for the grid voltage and current vectors to be in phase. The reference active power is being supplied by the dc link voltage control. The voltage reference for the average conversion control method, which

regulates the switches of the grid inverter, is established by the output of the current controllers. [30], [32] and [37]. The DC link voltage is given by:

$$\frac{du_{dc}}{dt} = \frac{1}{C_{dc}}(i_{dc} - i_{ond}) \quad (9)$$

Where,

$$i_c^* = i_{dc} - i_{ond} \quad (10)$$

The reference active power injected to the electrical supply network is given by:

$$P_g^* = u_{dc}i_{dc} - u_{dc}i_c^* \quad (11)$$

The reference voltages are expressed by [34].

$$\begin{aligned} v_{d_ond}^* &= v_{dg}^* + v_{dg} - \omega_s L_t i_{qg} \\ v_{q_ond}^* &= v_{qg}^* + v_{qg} + \omega_s L_t i_{dg} \end{aligned} \quad (12)$$

In order to maintain a constant DC link voltage, it is feasible to employ a proportional integral corrector. It is characterized by the capacitor value and the dynamics of the regulation loop. The reference currents of a network, as expressed in the d-q frame, are derived from the equation outlined in the following table [30].

$$\begin{aligned} i_{dg}^* &= \frac{P_g^* v_{dg} + Q_g^* v_{qg}}{v_{dg}^2 + v_{qg}^2} \\ i_{qg}^* &= \frac{P_g^* v_{qg} - Q_g^* v_{dg}}{v_{dg}^2 + v_{qg}^2} \end{aligned} \quad (13)$$

2. DTC of Dual Stator Induction Generator

The DTC of a DSIG is based on errors between references and estimated torque and flow values to directly control inverter states to maintain torque and flow errors within band limits prefixed. For this purpose, tables are used to select the switching procedure based on the inverter states and maintain the influence of the parameter variation during operation [50]. The DTC contains a pair of hysteresis comparators, a torque and flux estimator, and a voltage vector selection table. Torque and flow are controlled simultaneously by applying appropriate tension vectors and limiting these amounts in their hysteresis bands [1], [47].

The stator flux, as given in equation (14), can be approximated as equation (15) over a short time period if the stator resistance is ignored [47]-[50].

$$\overline{\psi}_s = \overline{\psi}_{s0} + \int_0^t (\overline{V}_s - R_s \overline{I}_s) dt \quad (14)$$

$$\overline{\psi}_s \approx \overline{\psi}_{s0} + \int_0^t \overline{V}_s dt \quad (15)$$

During one period of sampling T_e , vector tension applied to the machine remains constant, and thus one can write:

$$\overline{\psi}_s(k+1) \approx \overline{\psi}_s(k) + \overline{V}_s \cdot T_e \quad (16)$$

$$\text{Or: } \Delta \overline{\psi}_s \approx \overline{V}_s \cdot T_e \quad (17)$$

Where: T_e : The sampling period in which the voltage vector is applied to the stator windings.

The stator flux ψ_s relates to the stator voltage vector V_s by equation (17) shows that the derivative of ψ_s reacts instantly to changes in V_s . The stator voltage V_s , in fact, the pulse width modulated output voltage of the MLI converter, which can be controlled by the reference vector V_{ref} in the spatial vector modulation V_{ref} . Since V_{ref} is synthesized by the voltage vectors (switching states) of the converter, proper selection of vectors can make the amplitude and angle of ψ_s adjustable [1], [37]. The expression of the electromagnetic torque is given by the following equation [60], [61].

$$T_{em} = k_c \cdot \|\vec{\psi}_s\| \cdot \|\vec{\psi}_r\| \sin(\theta) \quad (18)$$

Where, θ is the angle between the stator and rotor flux linkage, k_c is constant depending on the parameters of the machine, and $\vec{\psi}_s, \vec{\psi}_r$ are the stator and rotor flux space vectors

Besides, the switching table is depicted in Table 1. A two levels classical voltage inverter can achieve seven separate positions in the phase corresponding to the eight sequences of the voltage inverter [1], [47]-[49].

Direct torque control essence is to control the electromagnetic torque of the generator by adjusting the torque angle θ while maintaining the amplitude of the stator flux at a constant value (normally at its nominal value). Since the stator flux is maintained at its nominal value, the generator's ψ_r rotor flux is almost constant, varying only a few percent around its nominal value over a wide operating range. As a result, the torque can be controlled directly by θ [1], [63] and [64]. Different vectors of stator voltages provided by a two levels inverter shown in Fig. 2. The Direct Torque of DFIG shown in Fig. 3.

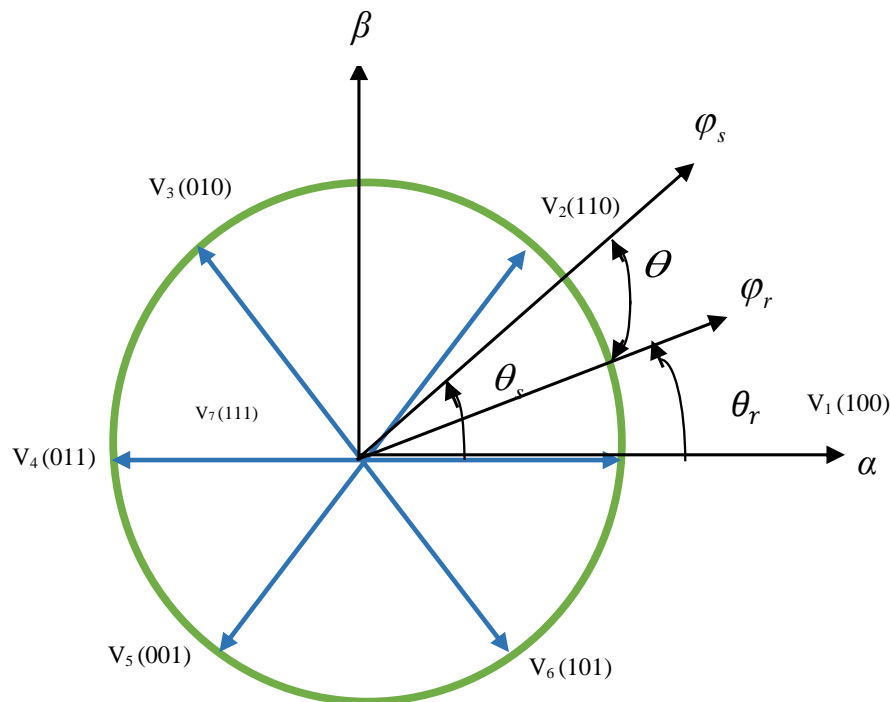


Fig. 2. Different vectors of stator voltages provided by a two levels inverter

Table 1. Vectors voltage localization

$\Delta\phi_s$	ΔT	S1	S2	S3	S4	S5	S6
0	1	110	010	011	001	001	100
	0	000	000	000	000	000	000
	-1	101	100	110	010	010	001
	1	010	011	001	101	100	110
1	0	000	000	000	000	000	000
	-1	001	101	100	110	010	011

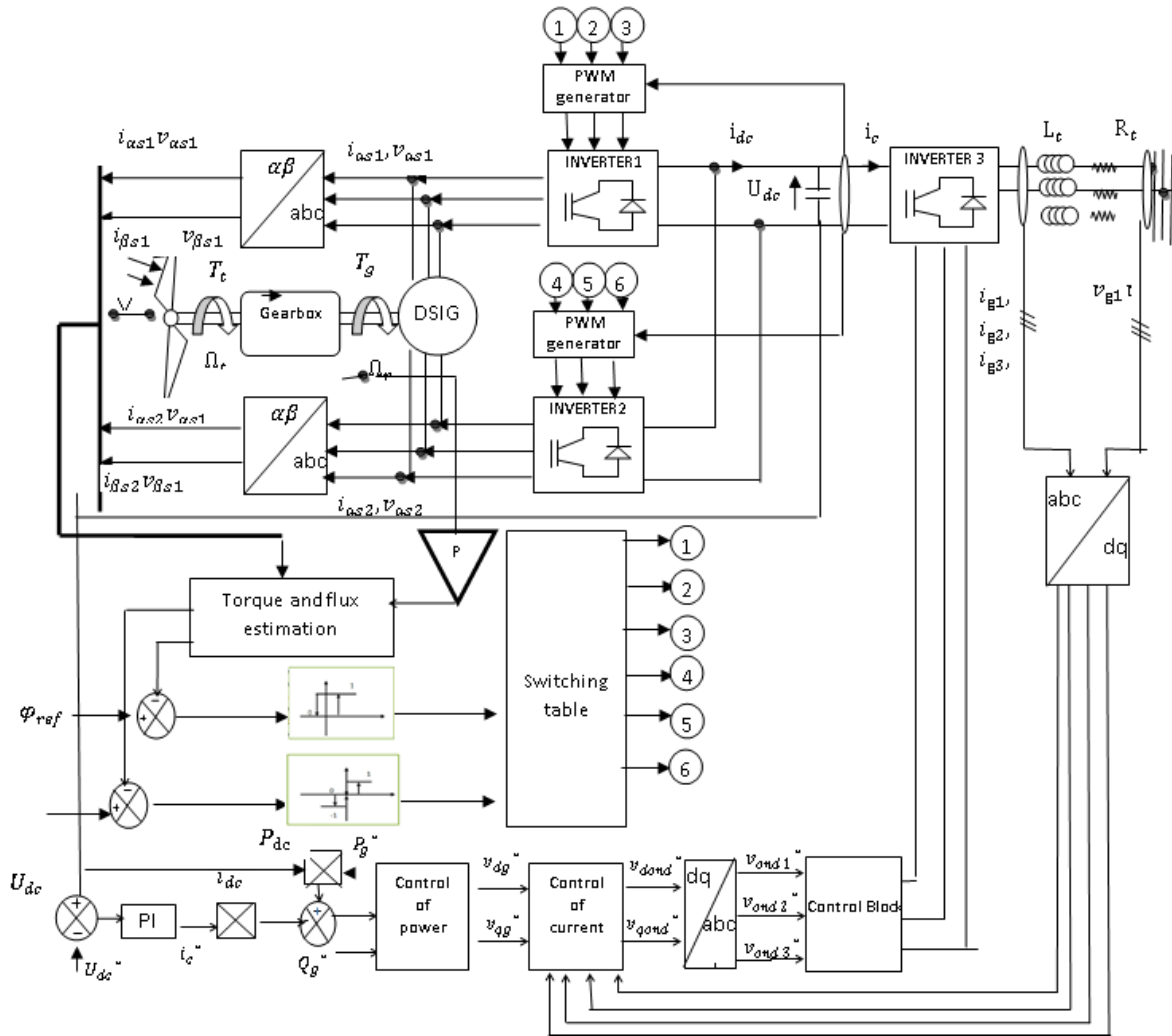


Fig. 3. The direct torque of DSIG

3. Discussion Simulation Results

The computer simulation results for a 1.5 MW DSIG using a PI controller under two different wind speed profiles (constant and random) were examined in order to confirm the validity of the suggested controller. The Appendix contains the test DSIG parameters that were used in the simulation.

The results of simulations are obtained for reactive power $Q=0$ and DC link voltage $U_{dc} = 1130$ V: one can note from Fig. 5, The speed of the machine follows its reference from the first value of 135(rad/s), up to the value of 139.6 (rad/s), it takes the same wind speed (see Fig. 4). In Fig. 6 the electromagnetic torque follows its reference and its estimate, and oscillates with a slightly large ripple rate, while the torque changes its value about -2205 (N.m), at the end value of -2384(N.m); From Fig. 7 the active power continues its reference, and varies from -0.6208 (MW) and -0.7100 (MW),

An improvement in the tip speed λ and the power coefficient C_p for which there is a decrease in fluctuations around their optimal values (9 for tip speed and 5.2 for coefficient power), in all the time of wind profile (see Fig. 8 and Fig. 9). In Fig. 10, the evolution of the flow in the two-phase (α , β), stator is circular; It can be seen that the stator flow established at the reference value 1.27 (see Fig. 11); Fig. 12 shows a sinusoidal form of the stator phase voltage and current and 180° phase shift between them, which reflects the production of electrical energy. The effective value of the phase

voltage 435 (V) and the effective value of the phase current varies from 280 (A) and 296 (A); It can see from Fig. 13, the DC link voltage is maintained at a constant level (1130 V), From Fig. 14 the grid voltage and current have the sinusoidal and 180° phase shift form between them, this justifies that the power flow is always from the aerogenerator to the electric grid. the effective value of the 563 (V) phase voltage and the effective value of the phase current varies from 552 (A) and 668 (A), the peak value of grid current is a dual one for the stator current, this justified that there are two stators. Hence that the real power extracted from the wind energy conversion systems can pass through the grid. Fig. 15 illustrates, the active and reactive powers supplied to the grid, where the active power varies from -0.6357 (MW) and -0.7114 (MW), and the reactive power is zero according to its imposed set point (a negative power represents a generated power). From these simulations, one can notice the performances of the DTC control which ensure a decoupling, similar to that obtained by the vector control which adequately ensured the MPPT of the wind system. To bring the reality, it was applied a wind speed profile in form of random (see Fig. 16). From Fig. 17, Fig. 18, Fig. 19, Fig. 20, Fig. 21, Fig. 22, Fig. 23, Fig. 24, Fig. 25, Fig. 26, Fig. 27 good results are obtained under both transient and steady state conditions.

The wind power captured and DSIG speed follow properly their optimal reference and have the same waveform as applied wind profile. The electromagnetic torque converges quickly to its reference. The active power tracks quite well its set-point up to the rated speed and extracts the maximum power, when the reactive power is fixed to 0 VAR. From the stator voltage and current waveforms, it can be seen that, the stator operates nearly at unity power factor.

In order to highlight the robustness of the suggested DTC control with respect to stator resistance variation (R_s), the simulation tests were performed taking into account the increase and decrease of this parameter. The results are shown in Fig. 28, Fig. 29, Fig. 30, Fig. 31. It can be noted that the velocity and flow dynamics and are not affected by the variation of the stator resistance. This shows the robustness of the suggested control algorithm.

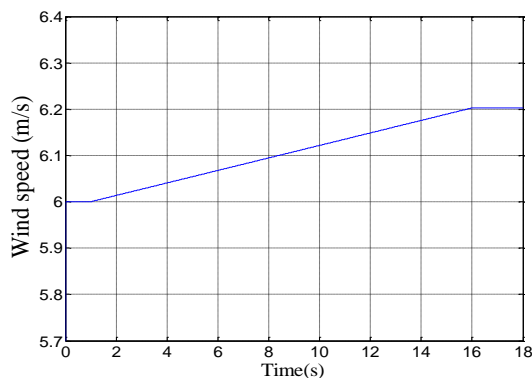


Fig. 4. The wind speed profile

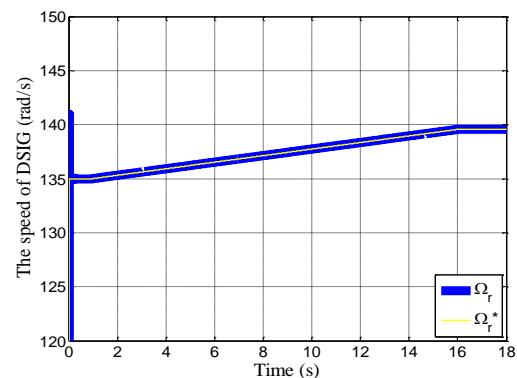


Fig. 5. The Speed of DSIG

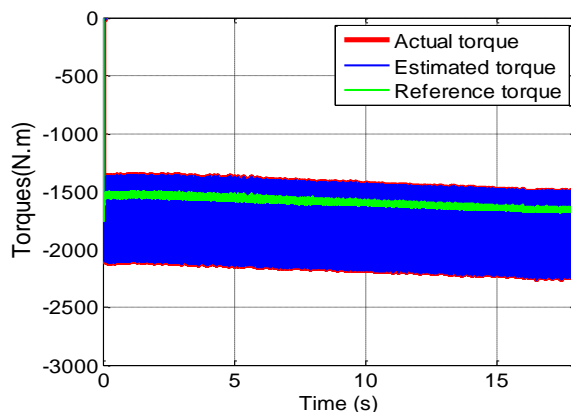


Fig. 6. The torque of DSIG

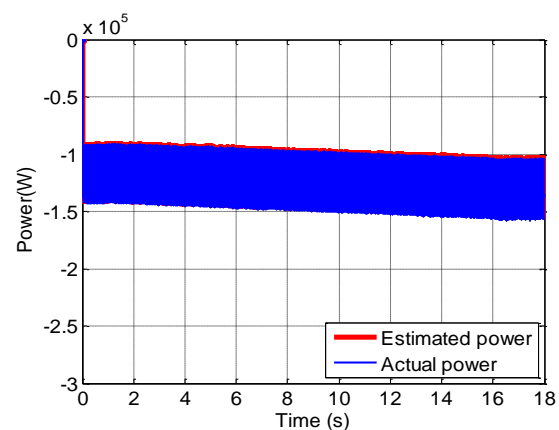


Fig. 7. The power of DSIG

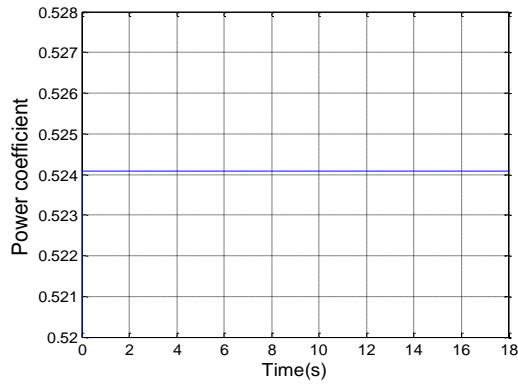


Fig. 8. The power coefficient

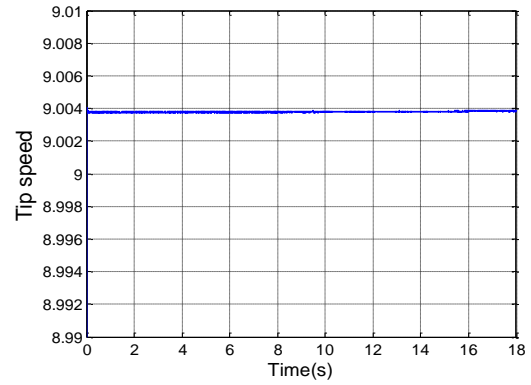


Fig. 9. The tip speed

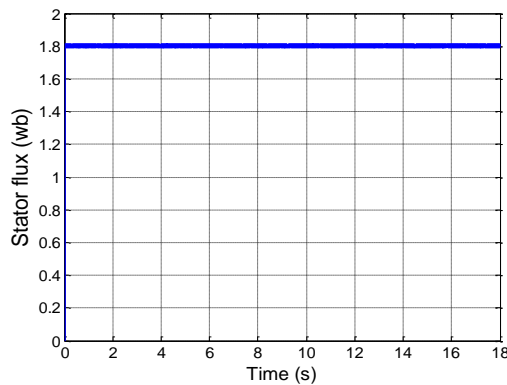


Fig. 10. The stator flux

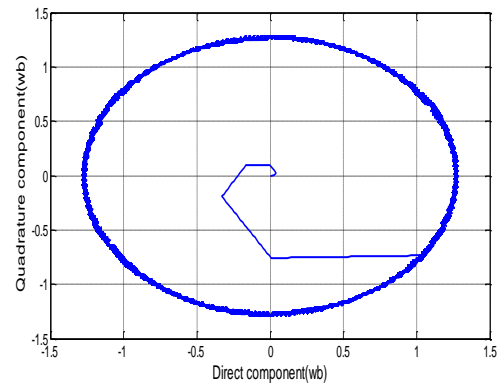


Fig. 11. The evolution of the stator flux

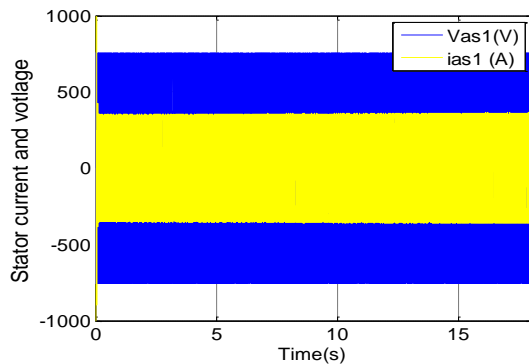


Fig. 12. The stator current and voltage

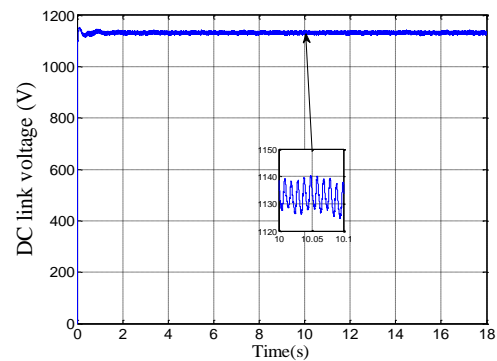


Fig. 13. DC link voltage

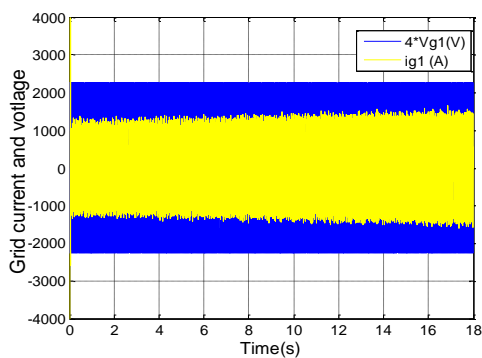


Fig. 14. The grid voltage and current

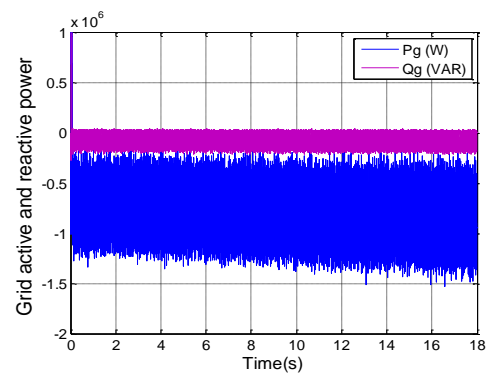


Fig. 15. The grid active and reactive power

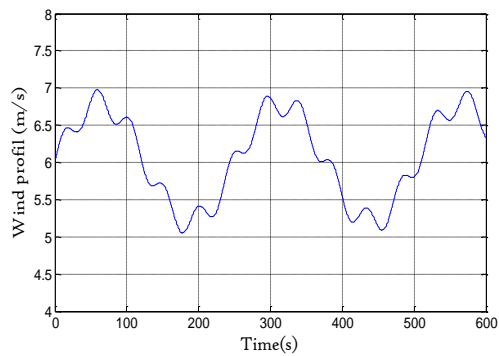


Fig. 16. The wind speed profile

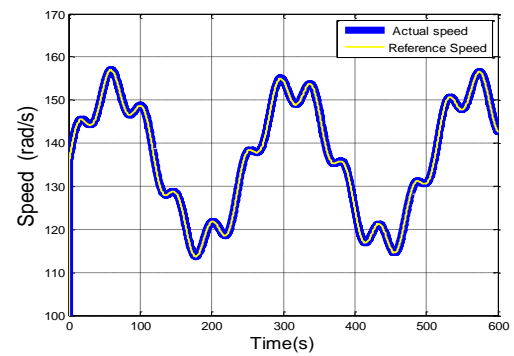


Fig. 17. DSIG speed

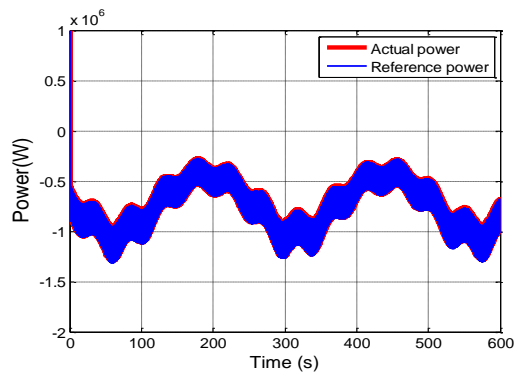


Fig. 18. Torque of DSIG

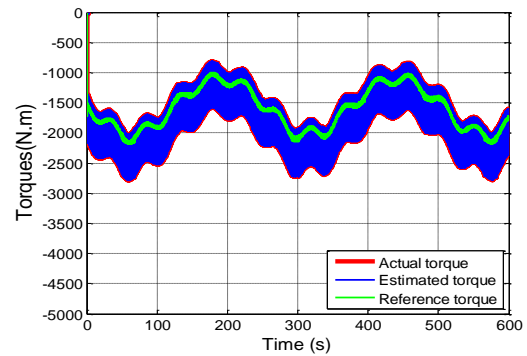


Fig. 19. Stator active power

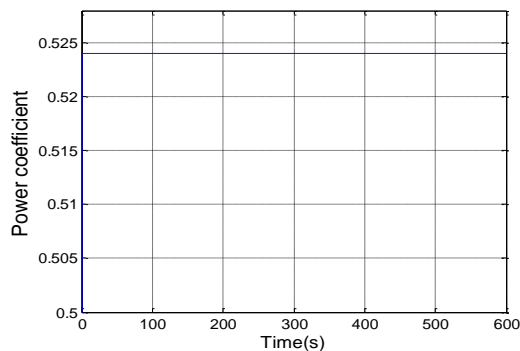


Fig. 20. The power coefficient

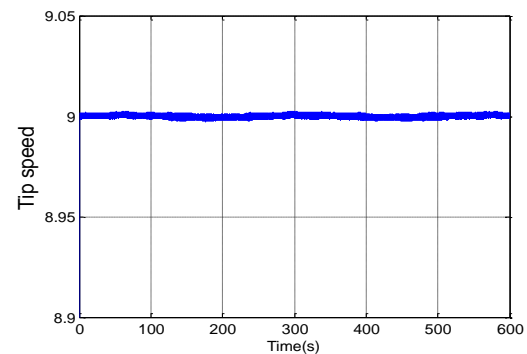


Fig. 21. The tip speed

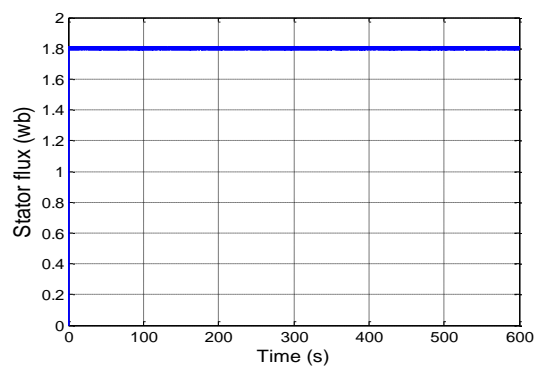


Fig. 22. The stator flux

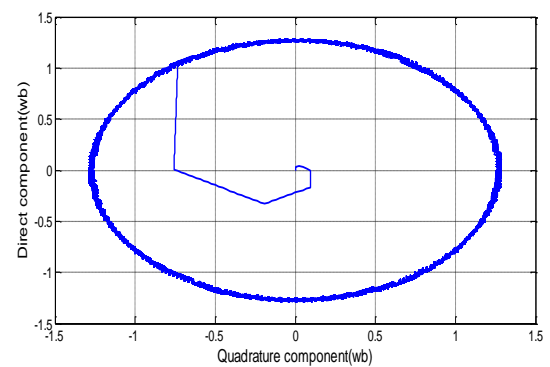


Fig. 23. The Evolution of the stator flux

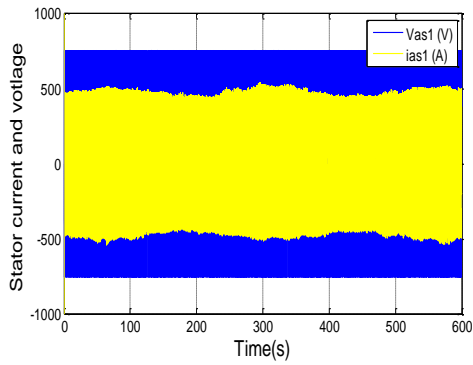


Fig. 24. The stator voltage and current

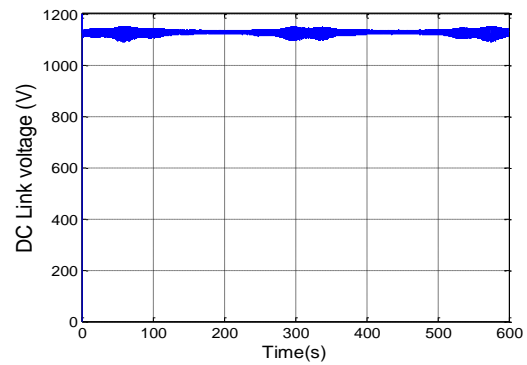


Fig. 25. The DC link voltage

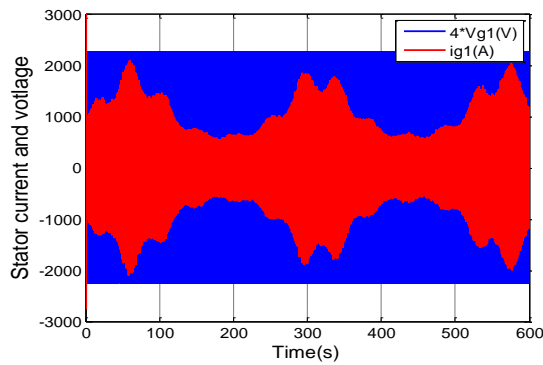


Fig. 26. The grid voltage and current

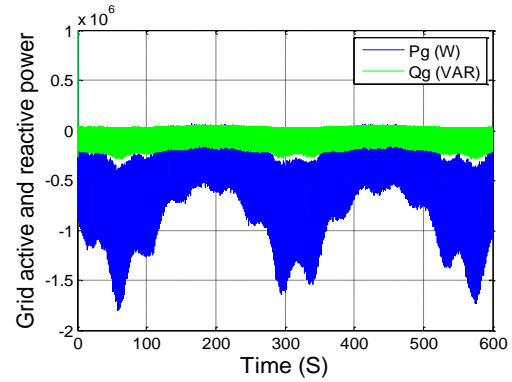


Fig. 27. The grid active and reactive power

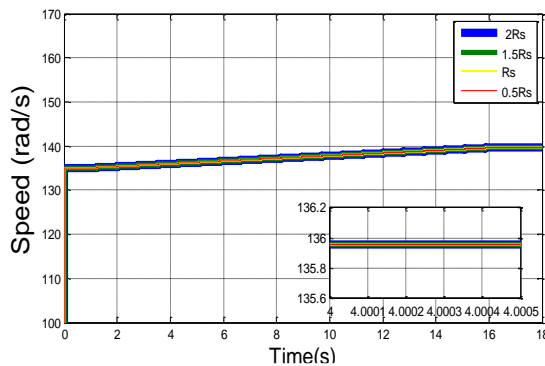


Fig. 28. The wind speed profile

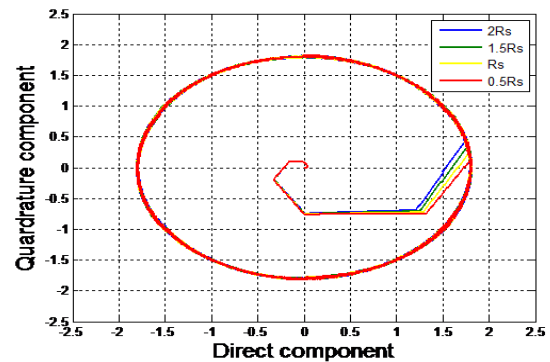


Fig. 29. The evolution of the stator flux

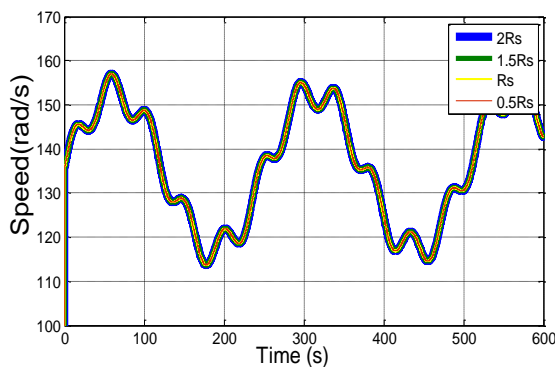


Fig. 30. The wind speed profile

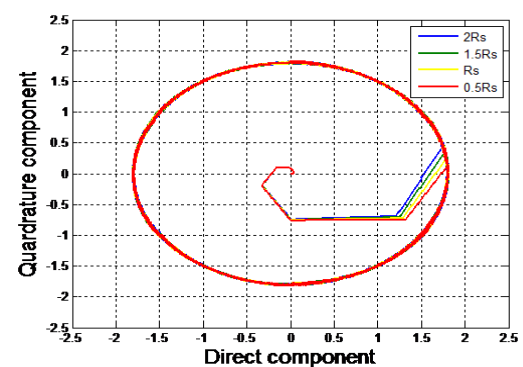


Fig. 31. The evolution of the stator flux

4. Conclusion

In this paper, a direct torque flux control algorithm for a two-stator induction generator in a wind energy conversion system based on a grid-connected DSIG is proposed. The performance of the proposed system was simulated under different conditions such as wind speed profile changes and parameter variations. This proves that DTFC is not only robust but can also improve the dynamic performance of the system. The proposed DTFC method achieves.

- Good pursuit of reference speed;
- The DTC is fast response compared with vector control [27], [37].
- Good support for turbine and generator parameter variation and power grid disturbances.

The work done opens up several perspectives. Some of the issues that have not been discussed here in detail and may be the subject of future research include:

- The practical realization of DTC control
- DSIG study associated with matrix and multilevel inverters
- Integration of DSIG in a mixed wind farm;

Author Contribution: All authors contributed equally to the main contributor to this paper. All authors read and approved the final paper.

Funding: This research received no external funding.

Conflicts of Interest: The authors declare no conflict of interest.

Parameters

Turbine: Diameter = 60 m, Number of blades = 3, Hub height = 85 m, Gearbox = 90

DSIG: 1.5 MW, 400 V, 50 Hz, 2 pole pairs, $R_{s1}=R_{s2}=0.008 \text{ X}$, $L_1=L_2=0.134 \text{ mH}$, $L_m=0.0045 \text{ H}$, $R_r=0.007 \text{ X}$, $L_r=0.067 \text{ mH}$, $J=104 \text{ kg m}^2$ (turbine + DSIG), $f_r=2.5 \text{ N m s/rd}$: (turbine + DSIG).

Nomenclature

G	Gear ratio
V	Wind velocity
P_n	Nominal power
S	Area of the rotor
λ	Tip speed ratio
λ_{opt}	The optimal Tip speed ratio
C_p	Power coefficient
C_{pmax}	The maximum power coefficient
Ω_r	Mechanical speed of the DSIG
Ω_r^*	Mechanical speed reference
Ω_t	Turbine speed
T_t	Aerodynamic torque
T_g	Generator torque
R_{s1}, R_{s2}	Per phase stators resistances

L_1, L_2	Per phase stators leakages inductances
L_m	Magnetizing inductance
R_r	Per phase rotor resistance
L_r	Per phase rotor leakage inductances
J	Inertia (turbine + DSIG),
f_r	Viscous coefficient
P	Number of pole pairs
t_f	final time
ω_s	Speed of the synchronous reference frame
ω_r	Rotor electrical angular speed
ω_{gl}	Sliding speed
T_{em}	Electromagnetic torque
T_{em}^*	Electromagnetic torque reference
$V_{qs1}, V_{ds1}, V_{qs2}, V_{ds2}$	“d–q” stators voltages
$v_{d1}^*, v_{q1}^*, v_{d2}^*, v_{q2}^*$	“d–q” stators voltages references
$i_{ds1}, i_{qs1}, i_{ds2}, i_{qs2}$	“d–q” stators currents
V_{qr}, V_{dr}	“d–q” rotor voltages
I_{qr}, I_{dr}	“d–q” rotor currents
ϕ_r^*	Flux reference
U_{dc}	DC Link voltage
U_{dc}^*	DC Link voltage reference
Q_g	Grid reactive power
P_g	Grid active power
Q_g^*	Grid reactive power reference
P_g^*	Grid active power reference
v_{dg}^*, v_{qg}^*	“d–q” grid voltages
v_{dg}, v_{qg}	“d–q” grid voltages references
i_{dg}, i_{qg}	“d–q” grid currents
i_{dg}^*, i_{qg}^*	“d–q” grid currents references

References

- [1] B. Wu, Y. Lang, N. Zargari, S. Kouro, “Power conversion and control of wind energy systems,” *John Wiley & Sons*, vol. 74, 2011, <https://doi.org/10.1002/9781118029008>.
- [2] D. K. Bhutto, J. Ahmed Ansari, S. S. Hussain Bukhari and F. Akhtar Chachar, “Wind Energy Conversion Systems (WECS) Generators: A Review,” *2019 2nd International Conference on Computing, Mathematics and Engineering Technologies (iCoMET)*, pp. 1-6, 2019, <https://doi.org/10.1109/ICOMET.2019.8673429>.

-
- [3] A. Akinrinde, A. Swanson, R. Tiako, "Dynamic Behavior of Wind Turbine Generator Configurations during Ferroresonant Conditions," *Energies*, vol. 12, no. 4, p. 639, 2019, <https://doi.org/10.3390/en12040639>.
- [4] A. Adjati, "Etude des machines asynchrones à double étoile en pompage hybride à énergies renouvelables," *Doctoral dissertation, Université de Béjaia-Abderrahmane Mira*, 2022, <https://www.pnst.cerist.dz/detail.php?id=889124>.
- [5] A. R. Soman, "Design And Development of Dual Stator Induction Machine," *Independent Author*, 2023, https://books.google.co.id/books/about/Design_and_Development_of_Dual_Stator.
- [6] H. Liu *et al.*, "Control Strategy for Five-Phase Dual-Stator Winding Induction Starter/Generator System," *IEEE Transactions on Industrial Electronics*, vol. 67, no. 4, pp. 2607-2617, 2020, <https://doi.org/10.1109/TIE.2019.2912767>.
- [7] A. R. Soman, R. M. Holmukhe, "Double Stator Induction Machine for Variable Speed And Variable Torque Applications," *International Journal of Electrical and Electronics Engineering*, vol. 8, no. 12, pp. 1-4, 2021, <https://doi.org/10.14445/23488379/IJEEE-V8I12P101>.
- [8] J. I. Talpone, P. F. Puleston, M. G. Cendoya, J. A. Barrado-Rodrigo, "A Dual-Stator Winding Induction Generator Based Wind-Turbine Controlled via Super-Twisting Sliding Mode," *Energies*, vol. 12, no. 23, p. 4478, 2019, <https://doi.org/10.3390/en12234478>.
- [9] K. Hamitouche, S. Chekkal, H. Amimeur, D. Aouzellag, "A new control strategy of dual stator induction generator with power regulation," *Journal Européen des Systèmes Automatisés*, vol. 53, no. 4, pp. 469-478, 2020, <https://doi.org/10.18280/jesa.530404>.
- [10] M. Benadja and A. Chandra, "A new MPPT algorithm for PMSG based grid connected wind energy system with power quality improvement features," *2012 IEEE Fifth Power India Conference*, pp. 1-6, 2012, <https://doi.org/10.1109/PowerI.2012.6479531>.
- [11] R. Pena, R. Cardenas, R. Blasco, G. Asher and J. Clare, "A cage induction generator using back to back PWM converters for variable speed grid connected wind energy system," *IECON'01. 27th Annual Conference of the IEEE Industrial Electronics Society (Cat. No.37243)*, vol. 2, pp. 1376-1381, 2001, <https://doi.org/10.1109/IECON.2001.975982>.
- [12] M. S. ElMoursi, "Automatic Gain Controller for Variable Speed Wind Turbines," *International Journal of Emerging Electric Power Systems*, vol. 9, no. 1, 2008, <https://doi.org/10.2202/1553-779X.1558>.
- [13] A. G. Abo-Khalil, D. Lee and J. Seok, "Variable speed wind power generation system based on fuzzy logic control for maximum output power tracking," *2004 IEEE 35th Annual Power Electronics Specialists Conference (IEEE Cat. No.04CH37551)*, vol. 3, pp. 2039-2043, 2004, <https://doi.org/10.1109/PESC.2004.1355431>.
- [14] M. Goyal, Y. Fan, A. Ghosh and F. Shahnia, "Techniques for a Wind Energy System Integration with an Islanded Microgrid," *International Journal of Emerging Electric Power Systems*, vol. 17, no. 2, pp. 191-203, 2016, <https://doi.org/10.1515/ijeeps-2015-0139>.
- [15] S. Li, T. A. Haskew, R. Chaloo, "Steady-State Characteristic Study for Integration of DFIG Wind Turbines into Transmission Grid," *International Journal of Emerging Electric Power Systems*, vol. 10, no. 1, 2009, <https://doi.org/10.2202/1553-779X.1967>.
- [16] M. Lope, "Contribution A L'optimisation D'un Systeme De Conversion Eolien Pour Une Unite De Production Isolee," *Energie électrique*, 2008, <https://theses.hal.science/tel-00344978v1>.
- [17] N. S. Barakin, N. I. Bogatyrev and A. A. Kumeyko, "Asynchronous Generator with Winding Capable of Switching Between double Star and Star-Triangle Forms," *2019 International Russian Automation Conference (RusAutoCon)*, pp. 1-5, 2019, <https://doi.org/10.1109/RUSAUTOCON.2019.8867693>.
- [18] T. Senjyu *et al.*, "Output power leveling of wind generation system using inertia of wind turbine," *2008 IEEE International Conference on Sustainable Energy Technologies*, pp. 1217-1222, 2008, <https://doi.org/10.1109/ICSET.2008.4747192>.
- [19] S. Li, T. A. Haskew, R. Chaloo, M. Nemmers, "Wind Power Extraction from DFIG Wind Turbines Using Stator-Voltage and Stator-Flux Oriented Frames," *International Journal of Emerging Electric Power Systems*, vol. 12, no. 3, 2011, <https://doi.org/10.2202/1553-779X.2676>.
-

-
- [20] A. Pratap, N. Urasaki, T. Senju, "Control Strategies for Smoothing of Output Power of Wind Energy Conversion Systems," *International Journal of Emerging Electric Power Systems*, vol. 14, no. 6, pp. 525-534, 2013, <https://doi.org/10.1515/ijeeps-2012-0030>.
- [21] D. Aouzellag, K. Ghedamsi, E. M. Berkouk, "Network Power Flux Control of a Wind Generator," *Renewable Energy*, vol. 34, no. 3, pp. 615-622, 2009, <https://doi.org/10.1016/j.renene.2008.05.049>.
- [22] I. Abdulwahab, A. S. Abubakar, A. Olaniyan, B. O. Sadiq and S. A. Faskari, "Control of Dual Stator Induction Generator Based Wind Energy Conversion System," *2022 IEEE Nigeria 4th International Conference on Disruptive Technologies for Sustainable Development (NIGERCON)*, pp. 1-5, 2022, <https://doi.org/10.1109/NIGERCON54645.2022.9803100>.
- [23] F. Lounas, S. Haddad, N. Benamrouche, "Active and Reactive Power Control of a Dual Stator Induction Machine (DSIM) using PI Controllers," *Indonesian Journal of Electrical Engineering and Informatics*, vol. 7, no. 4, pp. 664-676, 2020, <http://dx.doi.org/10.52549/ijeei.v7i4.1424>.
- [24] M. L. Khilfi, "Behaviour of a dual stator induction machine fed by neutral point clamped multilevel inverter," *Journal of Energy*, vol. 2018, 2018, <https://doi.org/10.1155/2018/6968023>.
- [25] F. Aymen, N. Mohamed, S. Chayma, C. H. R. Reddy, M. M. Alharthi and S. S. M. Ghoneim, "An Improved Direct Torque Control Topology of a Double Stator Machine Using the Fuzzy Logic Controller," *IEEE Access*, vol. 9, pp. 126400-126413, 2021, <https://doi.org/10.1109/ACCESS.2021.3110477>.
- [26] A. Adjati, T. Rekioua, D. Rekioua, A. Tounzi, "Study of dual stator induction motor in photovoltaic-fuel cell hybrid pumping Application," *Journal Européen des Systèmes Automatisés*, vol. 53, no. 5, pp. 601-608, 2020, <https://doi.org/10.18280/jesa.530502>.
- [27] A. Adjati, T. Rekioua, D. Rekioua, "Use of the Dual Stator Induction Machine in Photovoltaic Wind Hybrid Pumping," *Journal Européen des Systèmes Automatisés*, vol. 54, no. 1, pp. 115-124, 2021, <https://doi.org/10.18280/jesa.540113>.
- [28] D. Hadiouche, "Contribution à l'étude de la machine asynchrone double étoile: modélisation, alimentation et structure," *Doctoral dissertation, Université Henri Poincaré-Nancy 1*, 2001, <https://hal.univ-lorraine.fr/tel-01746497>.
- [29] G. K. Singh, K. B. Yadav, R. P. Saini, "Analysis of a Saturated Multi-Phase (Six- Phase) Self-Excited Induction Generator," *International Journal of Emerging Electric Power Systems*, vol. 7, no. 2, 2006, <https://doi.org/10.2202/1553-779X.1234>.
- [30] H. Amimeur, D. Aouzellag, R. Abdessemed, K. Ghedamsi, "Sliding mode control of a dual-stator induction generator for wind energy conversion systems," *International Journal of Electrical Power & Energy Systems*, vol. 42, no. 1, pp. 60-70, 2012, <https://doi.org/10.1016/j.ijepes.2012.03.024>.
- [31] M. Mahmud, S. M. A. Motakabber, A. H. M. Zahirul Alam and A. N. Nordin, "Adaptive PID Controller Using for Speed Control of the BLDC Motor," *2020 IEEE International Conference on Semiconductor Electronics (ICSE)*, pp. 168-171, 2020, <https://doi.org/10.1109/ICSE49846.2020.9166883>.
- [32] B. Meryem, B. Leila, A. Said and A. Fatima, "Robust control of a dual stator induction generator used in wind power generation," *2017 International Conference on Control, Automation and Diagnosis (ICCAD)*, pp. 174-179, 2017, <https://doi.org/10.1109/CADIAG.2017.8075652>.
- [33] G. K. Singh, K. Nam and S. K. Lim, "A simple indirect field-oriented control scheme for multiphase induction machine," *IEEE Transactions on Industrial Electronics*, vol. 52, no. 4, pp. 1177-1184, 2005, <https://doi.org/10.1109/TIE.2005.851593>.
- [34] E. Merabet, R. Abdessemed, H. Amimeur, F. Hamoudi, "Field oriented control of a dual star induction machine using fuzzy regulators," *Algorithms*, vol. 6, p. 12, 2007, <https://citeseerx.ist.psu.edu/document?repid=rep1&type=pdf&doi=cb47e3e7286547d76ab3981e73bb85d3ab2b398d>.
- [35] S. Chekkal, D. Aouzellag, K. Ghedamsi and H. Amimeur, "New control strategy of wind generator based on the dual-stator induction generator," *2011 10th International Conference on Environment and Electrical Engineering*, pp. 1-4, 2011, <https://doi.org/10.1109/EEEIC.2011.5874593>.
-

-
- [36] K. Kouzi, F. Ameer, K. M. Nachida, "Optimization Fuzzy Speed Vector Control of Dual Stator Induction Generator System Applied in Wind Power Generation System," *Journal of Electrical Engineering*, vol. 14, no. 1, p. 8, 2014, <http://jee.upt.ro/index.php/jee/article/view/WU1371188872W51baae884181f>.
- [37] Y. Ma and C. Kong, "Dissipative Asynchronous T-S Fuzzy Control For Singular Semi-Markovian Jump Systems," *IEEE Transactions on Cybernetics*, vol. 52, no. 6, pp. 5454-5463, 2022, <https://doi.org/10.1109/TCYB.2020.3032398>.
- [38] F. Ameer and K. Kouzi, "Genetic algorithm optimized PI and fuzzy logic speed vector control of Dual Stator Induction Generator in wind energy conversion system," *3rd International Conference on Systems and Control*, pp. 1036-1042, 2013, <https://doi.org/10.1109/ICoSC.2013.6750982>.
- [39] H. Amimeur, "Contribution au contrôle de la machine asynchrone double étoile," *Doctoral dissertation, Batna*, 2012, <https://www.ccdz.cerist.dz/admin/notice.php?id=00000000000000314082000000>.
- [40] H. Liu, F. Bu, W. Huang, H. Xu, M. Degano and C. Gerada, "Control-Winding Direct Power Control Strategy for Five-Phase Dual-Stator Winding Induction Generator DC Generating System," *IEEE Transactions on Transportation Electrification*, vol. 6, no. 1, pp. 73-82, 2020, <https://doi.org/10.1109/TTE.2019.2962635>.
- [41] K. Kouzi, L. Mokrani and M. S. Nait, "High performances of fuzzy self-tuning scaling factor of PI fuzzy logic controller based on direct vector control for induction motor drive without flux measurements," *2004 IEEE International Conference on Industrial Technology, 2004. IEEE ICIT '04*, vol. 2, pp. 1106-1111, 2004, <https://doi.org/10.1109/ICIT.2004.1490232>.
- [42] Y. Zeng, M. Cheng, X. Wei and G. Zhang, "Grid-Connected and Standalone Control for Dual-Stator Brushless Doubly Fed Induction Generator," *IEEE Transactions on Industrial Electronics*, vol. 68, no. 10, pp. 9196-9206, 2021, <https://doi.org/10.1109/TIE.2020.3028824>.
- [43] A. Iqbal and G. K. Singh, "PSO based controlled six-phase grid connected induction generator for wind energy generation," *CES Transactions on Electrical Machines and Systems*, vol. 5, no. 1, pp. 41-49, 2021, <https://doi.org/10.30941/CESTEMS.2021.00006>.
- [44] Y. Bendjeddou, R. Abdessemed, and E. Merabet, "Improved field oriented control for standalone dual star induction generator used in wind energy conversion," *Engineering Review*, vol. 40, no. 2, pp. 34-46, 2020, <https://doi.org/10.30765/er.40.2.05>.
- [45] S. Gao, H. Zhao, Y. Gui, D. Zhou and F. Blaabjerg, "An Improved Direct Power Control for Doubly Fed Induction Generator," *IEEE Transactions on Power Electronics*, vol. 36, no. 4, pp. 4672-4685, 2021, <https://doi.org/10.1109/TPEL.2020.3024620>.
- [46] K. Kouzi, L. Mokrani and M. S. Nait-Said, "A new design of fuzzy logic controller with fuzzy adapted gains based on indirect vector control for induction motor drive," *Proceedings of the 35th Southeastern Symposium on System Theory*, 2003, pp. 362-366, 2003, <https://doi.org/10.1109/SSST.2003.1194592>.
- [47] P. Vas, "Sensorless Vector and Direct Torque Control," *Oxford University Press*, vol. 2, pp. 265-273, 1998, <https://doi.org/10.1093/oso/9780198564652.001.0001>.
- [48] A. H. Niasar, H. R. Khoei, "Sensorless Direct Power Control Of Induction Motor Drive Using Artificial Neural Network," *Advances in Artificial Neural Systems*, vol. 2015, 2015, <https://doi.org/10.1155/2015/318589>.
- [49] M. T. Lamchich, "Torque Control," *InTech*, 2011, <https://doi.org/10.5772/636>.
- [50] F. Ameer, K. Kouzi, N. K. Merzouk, "Design and Analysis of Direct Power and Flux Control of Dual Stator Induction Generator Integrated in Wind Conversion System connected to the Grid," *Electrotehnică, Electronică, Automatică*, vol. 64, no. 3, 2016, <https://eea-journal.ro/ro/2016/eea-2016-64-3-047-en.pdf>.
- [51] M. M. Chowdhury, "Modelling And Control Of Direct Drive Variable Speed Wind Turbine With Interior Permanent Magnet Synchronous Generator," *University of Tasmania Open Access Repository*, 2014, <https://figshare.utas.edu.au/articles/thesis>.
- [52] G. S. Buja and M. P. Kazmierkowski, "Direct torque control of PWM inverter-fed AC motors - a survey," *IEEE Transactions on Industrial Electronics*, vol. 51, no. 4, pp. 744-757, 2004, <https://doi.org/10.1109/TIE.2004.831717>.
-

-
- [53] A. Nazari and H. Heydari, "A Novel Model-Based Predictive Direct Power Control of Doubly-Fed Induction Generator," *International Journal of Computer and Electrical Engineering*, vol. 4, no. 4, pp. 493-498, 2012, <http://dx.doi.org/10.17706/IJCEE>.
- [54] A. H. Niasar and H. R. Khoei, "Direct Power Control of Induction Motor Drive," *Journal of Power Electronics & Power Systems*, vol. 4, no. 2, pp. 48-55, 2014, <https://engineeringjournals.stmjournals.in/index.php/JoPEPS/article/view/3171>.
- [55] A. A. Hassan, A. M. El-Sawy, O. M. Kamel, "Direct Torque Control of A Doubly Fed Induction Generator Driven By A Variable Speed Wind Turbine," *Journal of Engineering Sciences*, vol. 41, no. 1, pp. 199-216, 2013, <https://dx.doi.org/10.21608/jesaun.2013.114703>.
- [56] L. Xu and P. Cartwright, "Direct active and reactive power control of DFIG for wind energy generation," *IEEE Transactions on Energy Conversion*, vol. 21, no. 3, pp. 750-758, 2006, <https://doi.org/10.1109/TEC.2006.875472>.
- [57] L. Benalia, A. Chaghi and R. Abdessemed, "Comparative Study Between A Double Fed Induction Machine And Double Star Induction Machine Using Direct Torque Control DTC," *Acta Universitatis Apulensis*, pp. 351-366, 2011, https://www.emis.de/journals/AUA/pdf/27_865_paper31-acta28-2011.pdf.
- [58] Z. Boudries, D. R. Ziani, and M. Sellami, "Direct power control of a PWM rectifier fed autonomous induction generator for wind energy applications," *Energy Procedia*, vol. 36, pp. 391-400, 2013, <https://doi.org/10.1016/j.egypro.2013.07.045>.
- [59] A. Mohan, M. Khalid and A. C. Binojkumar, "Performance Analysis of Permanent Magnet Synchronous Motor under DTC and Space Vector-based DTC schemes with MTPA control," *2021 International Conference on Communication, Control and Information Sciences (ICCISc)*, pp. 1-8, 2021, <https://doi.org/10.1109/ICCISc52257.2021.9484869>.
- [60] A. Chikhi, "Conception d'une Commande Floue Directe du Couple (FDTC) de la Machine Asynchrone Basée sur SVM," *Thèse de Doctorat de l'université de Batna*, 2013, <https://www.ccdz.cerist.dz/admin/notice.php?id=00000000000000314269000000>.
- [61] L. M. Tahar, L. Nora, "Direct Torque Control Based Multi-Level Inverter And Artificial Intelligence Techniques Of Induction Machine (DFIG)," *University Cadi Ayyad*, pp. 29-50, 2011, https://web.archive.org/web/20190503014052id_/https://cdn.intechopen.com/pdfs/13711.pdf.
- [62] X. Wang, Z. Wang, Z. Xu, M. Cheng and Y. Hu, "Optimization of Torque Tracking Performance for Direct-Torque-Controlled PMSM Drives With Composite Torque Regulator," *IEEE Transactions on Industrial Electronics*, vol. 67, no. 12, pp. 10095-10108, 2020, <https://doi.org/10.1109/TIE.2019.2962451>.
- [63] L. Salima, B. Tahar, S. Youcef, "Direct Torque Control Of Dual Star Induction Motor," *International Journal Of Renewable Energy Research*, vol. 3, no. 1, 2013, <https://www.ijrer.org/ijrer/index.php/ijrer/article/download/485/pdf>.
- [64] E. Benyoussef, S. Barkat, "Five-level Direct Torque Control with Balancing Strategy of Double Star Induction Machine," *International Journal of Systems Applications, Engineering & Development*, vol. 14, pp. 116-123, 2020, <https://doi.org/10.46300/91015.2020.14.16>.
-